

# Macular Microvasculature and Associated Retinal Layer Thickness in Pediatric Amblyopia: Magnification-Corrected Analyses

Noriko Nishikawa,<sup>1</sup> Jacqueline Chua,<sup>2-4</sup> Yuriya Kawaguchi,<sup>1</sup> Tomoko Ro-Mase,<sup>1</sup> Leopold Schmetterer,<sup>2-8</sup> Yasuo Yanagi,<sup>1-3</sup> and Akitoshi Yoshida<sup>1</sup>

<sup>1</sup>Department of Ophthalmology, Asahikawa Medical University, Asahikawa, Japan

<sup>2</sup>Singapore National Eye Centre, Singapore Eye Research Institute, Singapore

<sup>3</sup>Academic Clinical Program, Duke-NUS Medical School, National University of Singapore, Singapore

<sup>4</sup>SERI-NTU Advanced Ocular Engineering (STANCE), Singapore, Singapore

<sup>5</sup>Institute for Health Technologies, Nanyang Technological University, Singapore

<sup>6</sup>Department of Clinical Pharmacology, Medical University Vienna, Vienna, Austria

<sup>7</sup>Center for Medical Physics and Biomedical Engineering, Medical University Vienna, Vienna, Austria

<sup>8</sup>Institute of Molecular and Clinical Ophthalmology, Basel, Switzerland

Correspondence: Noriko Nishikawa, Department of Ophthalmology, Asahikawa Medical University, 2-1-1 Midorigaoka, Higashi, Asahikawa, Hokkaido, 078-8510, Japan; [nnori@asahikawa-med.ac.jp](mailto:nnori@asahikawa-med.ac.jp).

Received: November 22, 2020

Accepted: March 5, 2021

Published: March 30, 2021

Citation: Nishikawa N, Chua J, Kawaguchi Y, et al. Macular microvasculature and associated retinal layer thickness in pediatric amblyopia: Magnification-corrected analyses. *Invest Ophthalmol Vis Sci*. 2021;62(3):39. <https://doi.org/10.1167/iovs.62.3.39>

**PURPOSE.** The purpose of this study was to characterize macular microvasculature and structural retinal layers using magnification-corrected optical coherence tomography angiography (OCTA) images in children with amblyopia.

**METHODS.** This prospective cross-sectional study included 22 children with unilateral amblyopia (4–11 years of age) receiving spectral-domain OCTA. Vessel densities in foveal and parafoveal regions of the superficial capillary plexus (SCP) and deep capillary plexus (DCP) were measured in amblyopic and fellow eyes using a customized image analysis program correcting the scale of retinal image with axial length. Iowa Reference Algorithms (Iowa Institute for Biomedical Imaging) were used to measure mean thickness values of 10 intra-retinal layers rescaled for image size correction.

**RESULTS.** Foveal and parafoveal vessel densities in amblyopic eyes were lower than that of the fellow eyes in the SCP (fovea:  $P = 0.006$  and parafovea:  $P = 0.003$ ) and the DCP ( $P = 0.024$  and  $P = 0.025$ , respectively). Amblyopic eyes had significantly smaller foveal avascular zone (FAZ) area than fellow eyes ( $P < 0.001$ ). There were significant differences in retinal layer thickness between paired eyes, particularly in the inner retina in both foveal and parafoveal regions; retinal nerve fiber layer (RNFL) ( $P = 0.024$  and  $P = 0.095$ , respectively), ganglion cell layer ( $P < 0.001$  and  $P = 0.008$ ), inner plexiform layer (IPL;  $P = 0.12$  and  $P = 0.037$ ), inner nuclear layer ( $P = 0.005$  and  $P = 0.005$ ), and outer plexiform layer (OPL;  $P = 0.02$  and  $P = 0.057$ ), except in the foveal IPL, the parafoveal RNFL, and OPL.

**CONCLUSIONS.** Unilateral amblyopic eyes demonstrate reduced macular vessel density and thicker inner retinal layers compared with fellow eyes even after correcting for image magnification. Changes in macular microvasculature and structural layers may offer valuable insights in the development of amblyopia.

**Keywords:** amblyopia, microvasculature, retinal layer thickness, optical coherence tomography (OCT), optical coherence tomography angiography (OCTA)

Amblyopia is a common disease in which vision in one or both eyes does not develop properly during childhood due to refractive error differences, strabismus, visual form deprivation, or bilateral high refractive errors. Amblyopia was once considered a disorder of the visual cortex and lateral geniculate nucleus without structural abnormalities in the retina; however, since the advent of optical coherence tomography (OCT) and OCT angiography (OCTA), several studies have reported possible structural changes compared with normal eyes, including differences in macular thickness,<sup>1-4</sup> retinal nerve fiber layer (RNFL),<sup>1-3</sup> and individual

retinal layers,<sup>5,6</sup> and macular capillary vascular structure, including the foveal avascular zone (FAZ) area.<sup>7-12</sup>

Although these findings may provide novel insights to our understanding of amblyopia, they are now called into question. Specifically, measurements performed with OCT/OCTA have inherent errors when the scale of retinal image is not corrected for axial length (AL) of each eye.<sup>13-17</sup> Of note, a recent systematic review<sup>17</sup> reported that only 41 of 989 peer-reviewed articles (8%) in PubMed that use quantitative OCTA values used AL to correct the scale of OCTA images. This is particularly problematic in pediatric patients with

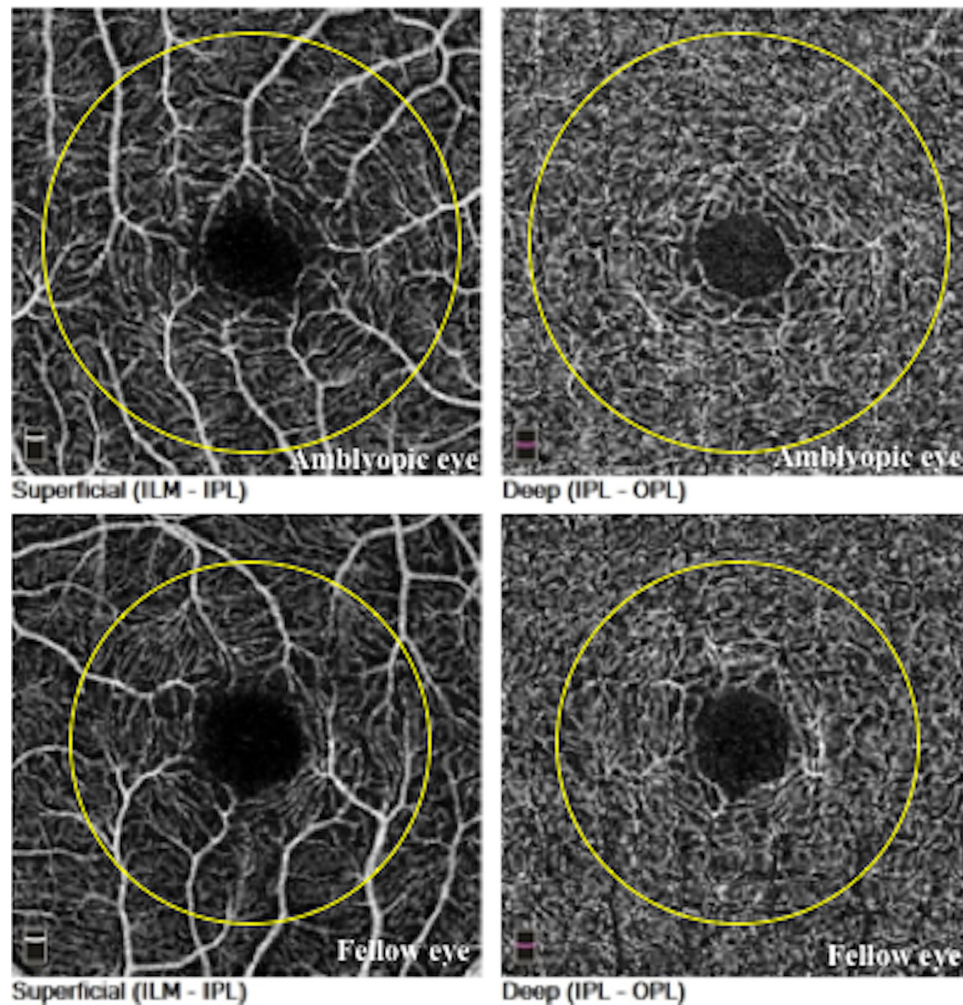


**FIGURE 1.** Typical spectral-domain optical coherence tomography angiography (OCTA) images. Example of macular (nominal scan area =  $3 \times 3$  mm) superficial and deep capillary plexus scans from an amblyopic eye (axial length of 21.89 mm) and the fellow eye (axial length of 23.45 mm). The *yellow circles* demarcate analysis regions (2.2 mm) corrected for axial length.

amblyopia, who may have significant differences in AL between the affected and unaffected eyes (especially those with anisometric amblyopia) and considering the fact that measurement of the FAZ area may deviate up to 51% if AL is not factored into the analysis.<sup>14</sup>

These findings prompted us to explore the argument regarding the structural abnormalities in eyes with amblyopia. For the current analysis, we accurately corrected for the magnifying effects on OCT/OCTA and clarified the abnormalities in the retinal structures and microvasculature in children with amblyopia.

## METHODS

This study was conducted in accordance with the principles of the Declaration of Helsinki and approved by the Institutional Review Board of Asahikawa Medical University. A written informed consent from the parents and an oral consent from the patients were obtained after providing a detailed explanation of the study objectives and protocol. This study was designed as a cross-sectional study and was conducted from January to November 2020.

Inclusion criteria were ages 4 to 15 years and a diagnosis of unilateral amblyopia due to anisometropia and anisometropia combined with strabismus (mixed-type). Patients were enrolled either at their initial visit, during treatment, or after successful treatment (obtaining visual acuity improvement). Only patients with best-corrected visual acuity (BCVA) of the fellow eye  $\geq 20/20$  were included. Exclusion criteria were the presence of other ocular diseases, systemic conditions known to influence vision (including diabetes, renal disease, and albinism), a history of ocular surgery, and premature birth. In addition, patients with foveal hypoplasia<sup>18</sup> or fragmented FAZ<sup>19</sup> detected via OCT/OCTA examination were excluded. All patients received a comprehensive ophthalmological examination, including BCVA, refractive error, slit lamp, funduscopy, and orthoptic evaluations. AL was examined using noncontact partial coherence interferometry (IOL Master 700; Carl Zeiss Meditec AG, Germany).

## OCTA Data Acquisition and Image Analysis

Macular images (nominal scan area =  $3 \times 3$  mm) were acquired using a spectral-domain OCT system with

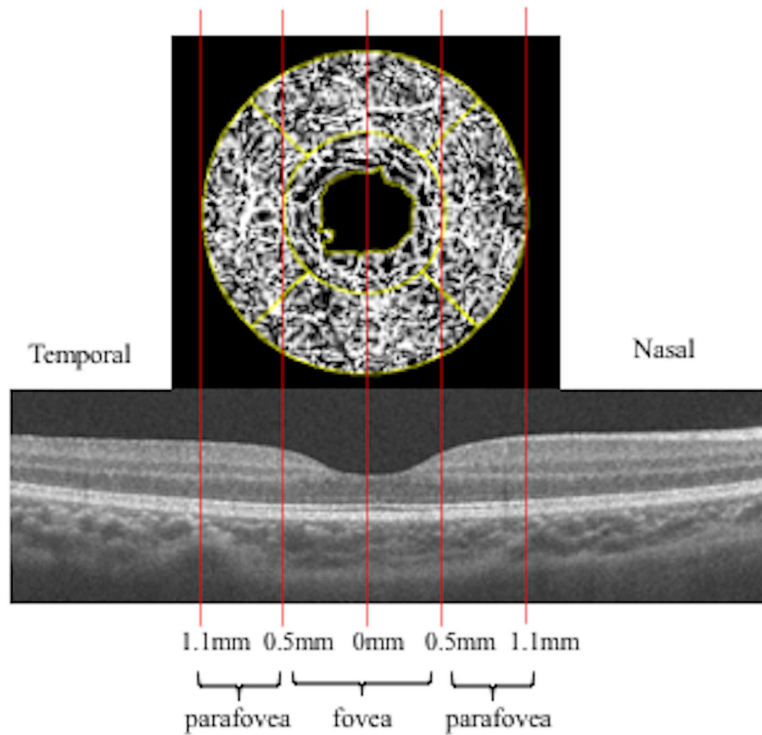


**FIGURE 2.** Diagram showing regions of interest. The fovea was defined by a circle 0.5 mm in diameter and the global parafovea by an annulus 0.5 to 1.1 mm in radius centered on the fovea. The parafoveal region was subdivided into superior, inferior, temporal, and nasal quadrants.

AngioVue software (RTVue XR Avanti; Optovue, Inc., Fremont, CA, USA). The Avanti OCT provides 70,000 A-scans/second to acquire OCT angiograms consisting of  $304 \times 304$  A-scans. Each OCT angiogram was created using orthogonal registration and merging two consecutive scan volumes. Each scan was then segmented into en face images of the superficial capillary plexus (SCP) and deep capillary plexus (DCP) using the autosegmentation feature of AngioVue (Fig. 1). SCP images were segmented with an inner boundary at the internal limiting membrane (ILM) and an outer boundary at  $9 \mu\text{m}$  above the inner plexiform layer (IPL). DCP images were segmented with an inner boundary  $9 \mu\text{m}$  above the IPL and an outer boundary  $9 \mu\text{m}$  below the outer plexiform layer (OPL).

The Littman and modified Bennett formulas were used to calculate true image size, as described previously.<sup>13,14,16</sup> Briefly, the relationship between the measured OCTA image diameter ( $D_m$ ) and the true diameter of the fundus ( $D_t$ ) could be expressed as  $D_t = p \times q \times D_m$ , where  $p$  is the magnification factor of the imaging system and  $q$  is a factor related to the eye ( $q = 0.01306 \times [AL - 1.82]$ ). For the Avanti systems used, the value of the magnification factor ( $p$ ) was 3.46, given a nominal AL of 23.95 mm.<sup>15</sup> Using this equation,  $D_t$  can be calculated based on scan size ( $D_m = 3 \text{ mm}$ ) area as  $D_t = 3.46 \times 0.01306 \times (AL - 1.82) \times 3$ .

### Vessel Density Analysis

Vessel density and FAZ area were calculated using the ImageJ/Fiji software (National Institutes of Health, Bethesda, MD, USA).<sup>20</sup> The ImageJ macro was developed to automatically correct for ocular magnification. In brief, the enface raw images ( $304 \times 304$  pixels) were imported and calcu-

lated the ocular magnification by substituting the AL as the above-mentioned equation using the code as shown below.

$$q = 0.01306 * (AL - 1.82);$$

>>> where AL = axial length

$$p = 3.46;$$

$$w = 304 / (p * q);$$

run ("Set Scale...", "distance = w known = 3  
unit = mm");

The superficial and deep images were merged into one image and rescaled to  $800 \times 800$  pixels using Bilinear interpolation. After binarization and skeletonization, we processed the image dilating and eroding repeatedly. The images were resized to originals and then the FAZ area and circularity index were measured similar to previous studies.<sup>12,21-23</sup> Regarding the vessel density analysis, the following processing was performed, with the foveal region being defined as a circular area with a radius of 0.5 mm and the parafoveal region as an annulus with a radius of 0.5 to 1.1 mm from the foveal center (Fig. 2). An actual 2.2-mm circle was cropped and the parafoveal region was subdivided into 4 quadrants (superior, inferior, temporal, and nasal). The SCP and DCP vessel density of each region was calculated from the binarized image, which used the Otsu method<sup>24</sup> as the percentage of the area defined as perfusion area<sup>21</sup> over the total area, excluding FAZ in the foveal region. To remove projection artifacts at the level of the DCP, a "mask" image of large superficial retinal vessels was created

TABLE 1. Demographic Characteristics of Patients

	Amblyopic Eye	Fellow Eye	P Value
Axial length, mm	21.68 (1.18)	22.57 (1.15)	0.015*
Refraction, diopter	4.94 (3.12 to 5.96)	1.31 (0.50 to 2.50)	<0.001†
BCVA, LogMAR	0.05 (−0.06 to 0.14)	−0.08 (−0.08 to −0.08)	<0.001†
Scan quality index	8.00 (8.00 to 8.75)	8.00 (7.00 to 8.00)	0.22†

BCVA, best-corrected visual acuity; LogMAR, logarithm of minimal angle resolution.

\* Paired t-test.

† Wilcoxon signed-rank test. Data were expressed as median (interquartile range).

from the corresponding SCP image, and the masked area was excluded from the analysis, as described in a previous study.<sup>25</sup>

### Individual Retinal Layer Thickness Analysis

Macular OCT images were imported into the Iowa Reference Algorithm (Retinal Image Analysis Lab, Iowa Institute for Biomedical Imaging, Iowa City, IA, USA),<sup>16,26,27</sup> which is an automated OCT layer segmentation algorithm used for individual retinal layer thickness analysis. All analyses were corrected for the magnification effect. Measurement methods for mean retinal thickness within the circular fovea region and annular parafoveal region were similar to those used for vessel density analysis. Individual thickness values were measured for (1) RNFL; (2) ganglion cell layer (GCL); (3) IPL; (4) inner nuclear layer (INL); (5) OPL; (6) outer nuclear layer (ONL); (7) photoreceptor inner/outer segments (IS/OS); (8) outer segment of photoreceptors; (9) outer segment photoreceptor/retinal pigment epithelium complex (OPR); and (10) retinal pigment epithelium (RPE). Total macular thickness was also calculated as the distance from the most anterior hyper-reflective line (corresponding to ILM) to the inner boundary of the RPE. For correlation analyses between vessel density and retinal layer thickness, the retina was stratified as a superficial layer (RNFL + GCL + IPL) and a deep layer (INL + OPL).

### Statistical Analysis

Statistical analyses were performed using EZR (Saitama Medical Center, Jichi Medical University, Saitama, Japan), a graphical user interface for R (The R Foundation for Statistical Computing, Vienna, Austria).<sup>28</sup> Visual acuity was converted to LogMAR for statistical calculations and analyses. Refraction data were converted into spherical equivalents. Vascular densities, FAZ parameters, and retinal layer thickness values were compared between amblyopic and fellow eyes using the paired sample *t*-test after confirming distribution normality using the Shapiro-Wilk test. Visual acuity (LogMAR) was compared between amblyopic and fellow eyes using the Wilcoxon signed-rank test. Associations between OCT and OCTA parameters as well as OCT/OCTA parameters and other clinical factors were evaluated using Pearson's correlation test or Spearman's correlation test, as applicable. Continuous variables are expressed as mean (standard deviation) for normally distributed data and median (interquartile range) for non-normally distributed data. Because the current study was exploratory, we performed the analysis without adjustment for multiple comparisons. All tests were two tailed and  $P < 0.05$  was considered statistically significant.

## RESULTS

### Demographic Data

This study examined 22 Japanese children with unilateral amblyopia (mean age = 8.1 (1.8) years, 9 boys); of these, 17 were diagnosed with anisometropic amblyopia and 5 with anisometropia combined with strabismus (mixed-type) amblyopia. Demographic and clinical parameters are summarized in Table 1. Amblyopic eyes had significantly poorer LogMAR visual acuity ( $P < 0.001$ ), were more hyperopic ( $P < 0.001$ ), and had shorter ALs ( $P = 0.015$ ) than fellow eyes.

### OCTA Parameters

Table 2 compares vessel density and FAZ parameters between amblyopic and fellow eyes. Amblyopic eyes had lower SCP vessel density (% areas) in foveal, global parafoveal, and all parafoveal quadrants compared with fellow eyes ( $P \leq 0.01$  for all), except in the temporal quadrant ( $P = 0.056$ ). Compared with fellow eyes, DCP vessel density was significantly lower in the fovea ( $P = 0.024$ ), the global parafovea ( $P = 0.025$ ), and the temporal quadrant ( $P = 0.018$ ) in the amblyopic eyes. In terms of FAZ, amblyopic eyes had a significantly smaller FAZ area than fellow eyes ( $P < 0.001$ ), but there was no difference in FAZ circularity index ( $P = 0.76$ ) between amblyopic and fellow eyes.

### OCT Parameters

The distribution of individual retinal layer thickness is shown in Table 3. Foveal and parafoveal macular thickness values were significantly greater in amblyopic eyes than in fellow eyes (foveal = 261.6 [19.30]  $\mu\text{m}$  vs. 253.8 [21.89]  $\mu\text{m}$ ,  $P < 0.001$ ; and parafoveal = 320.4 [13.56]  $\mu\text{m}$  vs. 316.0 [13.62]  $\mu\text{m}$ ,  $P = 0.007$ ). There were also significant differences in foveal and parafoveal GCL, INL, foveal RNFL, OPL, and parafoveal IPL thickness values between amblyopic and fellow eyes. There were no significant differences in outer retinal layer thickness values between amblyopic and fellow eyes, except that the parafoveal OPR thickness was significantly greater in the fellow eyes ( $P = 0.039$ ).

### Correlation Between OCT and OCTA Parameters

There were no significant correlations between foveal and global parafoveal SCP vessel densities and corresponding retinal thickness values (RNFL + GCL + IPL) or DCP vessel densities and corresponding retinal thickness values (INL + OPL) in both amblyopic and fellow eyes (all  $P$  values  $> 0.05$ ; data not shown).

**TABLE 2.** Comparison of Microvascular Parameters in Amblyopic and Fellow Eyes

		Amblyopic Eye	Fellow Eye	P Value
SCP (%)	Fovea	<b>41.15 (4.68)</b>	<b>43.62 (4.28)</b>	<b>0.006*</b>
	Parafovea (global)	<b>43.83 (4.85)</b>	<b>46.64 (4.57)</b>	<b>0.003*</b>
	Superior	<b>44.58 (5.12)</b>	<b>47.67 (4.39)</b>	<b>0.002*</b>
	Inferior	<b>43.98 (5.34)</b>	<b>47.2 (5.88)</b>	<b>0.007*</b>
	Nasal	<b>43.87 (4.66)</b>	<b>46.31 (4.10)</b>	<b>0.01*</b>
	Temporal	42.90 (5.34)	45.39 (5.49)	0.056
DCP (%)	Fovea	<b>53.96 (3.23)</b>	<b>55.71 (2.68)</b>	<b>0.024*</b>
	Parafovea (global)	<b>54.60 (3.45)</b>	<b>56.31 (2.52)</b>	<b>0.025*</b>
	Superior	55.54 (4.08)	57.34 (2.47)	0.05
	Inferior	54.49 (3.71)	55.74 (3.11)	0.116
	Nasal	54.52 (4.35)	56.36 (3.73)	0.10
	Temporal	<b>53.86 (3.06)</b>	<b>55.8 (2.84)</b>	<b>0.018*</b>
FAZ area, mm <sup>2</sup>	<b>0.22 (0.08)</b>	<b>0.24 (0.09)</b>	<b>&lt;0.001*</b>	
Circularity	0.58 (0.10)	0.58 (0.10)	0.76	

SCP, superficial capillary plexus; DCP, deep capillary plexus; FAZ, foveal avascular zone.

**TABLE 3.** Comparison of Individual Retinal Layer Thickness in Amblyopic and Fellow Eyes

Thickness, $\mu\text{m}$	Fovea			Parafovea (Global)		
	Amblyopic Eye	Fellow Eye	P Value	Amblyopic Eye	Fellow Eye	P Value
RNFL	<b>12.8 (3.07)</b>	<b>11.7 (3.12)</b>	<b>0.024*</b>	21.5 (1.84)	21.0 (1.64)	0.095
GCL	<b>23.1 (6.31)</b>	<b>20.4 (6.26)</b>	<b>&lt;0.001*</b>	<b>53.3 (4.41)</b>	<b>51.9 (3.86)</b>	<b>0.008*</b>
IPL	25.5 (4.25)	24.5 (5.32)	0.120	<b>40.4 (2.75)</b>	<b>39.6 (3.47)</b>	<b>0.037*</b>
RFNL + GCL + IPL	<b>61.3 (12.21)</b>	<b>56.6 (13.37)</b>	<b>&lt;0.001*</b>	<b>115.2 (7.26)</b>	<b>112.5 (7.70)</b>	<b>0.007*</b>
INL	<b>18.8 (3.02)</b>	<b>17.5 (2.87)</b>	<b>0.005*</b>	<b>37.5 (2.81)</b>	<b>36.4 (2.94)</b>	<b>0.005*</b>
OPL	<b>27.0 (4.73)</b>	<b>24.6 (5.04)</b>	<b>0.020*</b>	37.3 (4.99)	35.0 (4.72)	0.057
INL + OPL	<b>45.8 (6.18)</b>	<b>42.1 (6.84)</b>	<b>&lt;0.001*</b>	<b>74.8 (5.08)</b>	<b>71.4 (5.46)</b>	<b>0.018*</b>
ONL	107.6 (6.32)	107.6 (8.31)	0.97	89.8 (7.64)	91.0 (8.48)	0.35
IS OS	13.0 (0.62)	12.9 (0.64)	0.78	11.7 (0.44)	11.6 (0.50)	0.29
Outer segment of photoreceptors	15.8 (1.51)	16.0 (1.49)	0.28	11.9 (1.59)	11.9 (1.40)	0.99
OPR	18.1 (2.06)	18.6 (2.05)	0.122	<b>16.9 (2.02)</b>	<b>17.7 (1.89)</b>	<b>0.039*</b>
RPE	18.9 (1.69)	18.5 (1.59)	0.142	19.9 (1.86)	19.4 (1.98)	0.138
Macular thickness	<b>261.6 (19.30)</b>	<b>253.8 (21.89)</b>	<b>&lt;0.001*</b>	<b>320.4 (13.56)</b>	<b>316.0 (13.62)</b>	<b>0.007*</b>

Data were expressed as mean (standard deviation).

RNFL, retinal nerve fiber layer; GCL, ganglion cell layer; IPL, inner plexiform layer; INL, inner nuclear layer; OPL, outer plexiform layer; ONL, outer nuclear layer; IS OS, photoreceptor inner/outer segments; OPR, outer segment photoreceptor/retinal pigment epithelium complex; RPE, retinal pigment epithelium.

\* Total macular thickness was defined as layer 1 (retinal nerve fiber layer [RNFL]) to layer 9 (outer segment photoreceptor/retinal pigment epithelium complex; OPR).

### Correlation Between AL and OCT/OCTA Parameters, With or Without Image Magnification Correction

The results of the correlation analyses between AL and OCT/OCTA parameters, with and without image magnification correction, are shown in Supplementary Tables S1 and S2. Under image size correction, the thickness values of foveal and parafoveal RNFL (all  $P$  values  $< 0.003$ ), IPL (all  $P$  values  $\leq 0.011$ ), INL (all  $P$  values  $\leq 0.014$ ), and macular thickness (all  $P$  values  $\leq 0.014$ ) were negatively correlated with AL in both amblyopic and fellow eyes. Foveal GCL thickness was negatively correlated with AL in both amblyopic and fellow eyes (all  $P$  values  $< 0.001$ ). In fellow eyes, a negative correlation was observed between AL and foveal OPL and foveal and parafoveal RPE thickness (all  $P$  values  $< 0.04$  for all). Among the OCTA parameters, foveal and parafoveal DCP densities in both amblyopic and fellow eyes were positively correlated with AL (all  $P$  values  $< 0.01$ ). The FAZ area was positively correlated with AL in fellow eyes ( $P = 0.03$ ). When performing correlation analyses without image correction data, foveal RFNL, parafoveal ONL, and

OPR were negatively correlated with AL in amblyopic eyes (all  $P$  values  $< 0.03$ ), whereas foveal IPL, RPE, and macular thickness were negatively correlated with AL in fellow eyes (all  $P$  values  $< 0.04$ ). However, there was no correlation between AL and any of the OCTA parameters analyzed without image correction.

### Correlation Between OCT/OCTA Parameters and Other Clinical Factors

Supplementary Table S3 provides the results of correlation analysis between age and OCT parameters. Foveal and parafoveal outer segment of photoreceptor thickness in amblyopic eyes were positively correlated with age ( $r = 0.45$ ,  $P = 0.038$  and  $r = 0.52$ ,  $P = 0.013$ , respectively). In fellow eyes, foveal RNFL and OPL thickness were negatively correlated with age, whereas foveal ONL thickness was positively correlated with age. There were no correlations between age and any of the OCTA parameters in both amblyopic and fellow eyes ( $P > 0.05$  for all; data not shown). Visual acuity

in amblyopic eyes was not correlated with any OCTA parameter ( $P > 0.05$  for all; data not shown).

## DISCUSSION

OCT/OCTA enables noninvasive detailed visualization of retinal morphology and quantification of microvasculature metrics and retinal layer thickness. It has been known for a long time that AL of each eye affects the magnification of the retinal images and can affect the accuracy of the measurements. With the increased use of OCT/OCTA for the diagnosis and monitoring of various diseases, evaluating data from accurately corrected images is crucial to their interpretation. Odell et al.<sup>29</sup> found that the summed error of the nine Early Treatment Diabetic Retinopathy Study segments without magnification correction exceeded 20  $\mu\text{m}$  in 32% of the subjects. Sampson et al.<sup>14</sup> reported that image size correction in measurements of foveal superficial vessel density and FAZ area was  $> 5\%$  in 51% and 74% eyes, respectively. Some recent studies on amblyopia paid attention to magnification effect,<sup>4,10–12,30–32</sup> however, most of them merely used statistical adjustment to adjust the effects of AL along with other clinical factors.<sup>4,10,12,30,32</sup> In the current study, AL was significantly shorter in amblyopic eyes compared with the nonamblyopic fellow eyes, emphasizing the importance of AL adjustment in identifying disease-specific abnormalities in the retinal structure. Therefore, we corrected the image magnification of scans using ImageJ when analyzing FAZ parameters and vessel densities. Similarly, we analyzed retinal layer thickness values from the corresponding areas of magnification-corrected images using the automated Iowa Reference Algorithm.<sup>16</sup> To the best of our knowledge, this is the first report analyzing retinal microvasculature and corresponding retinal layer thickness in patients with amblyopia using OCT/OCTA images corrected for lateral magnification.

Several previous reports have found reduced SCP and DCP vessel densities in amblyopic eyes,<sup>7–9,32,33</sup> but another found only reduced SCP vessel density<sup>10</sup> and two others reported no changes.<sup>11,12</sup> Of these previous studies, one corrected for magnification effects using a built-in software,<sup>11</sup> three adjusted AL statistically,<sup>10,12,32</sup> and the others did not conduct or explicitly mention magnification correction.<sup>7–9,33</sup> One study that corrected for lateral scaling reported negative results, but the sample size was relatively small ( $n = 15$ ).<sup>11</sup> Additionally, projection artifact removal was not performed at the DCP level in these aforementioned studies, except one.<sup>10</sup> In the current analysis, foveal and global parafoveal SCP and DCP vessel densities were significantly lower in amblyopic eyes than in fellow eyes. These results concur with those of previous studies that did not correct image size for magnification error,<sup>7–9,33</sup> except for one study that did so, albeit only statistically.<sup>32</sup> Our results also confirm smaller FAZ area in amblyopic eyes than in fellow eyes; however, there were no significant differences in FAZ circularity. There are several possible explanations for the decreased vessel density in amblyopic eyes. First, decreased vessel density in amblyopic eyes might indicate that oxygen and nutrition demand decrease in the inner retina that receives blood supply from the retinal arterial system. Second, this may reflect an anomaly or delay during foveal development. Particularly, the fact that (1) the temporal quadrant at the level of DCP and (2) FAZ were decreased in the amblyopic eyes support this idea. Histologically, temporal retinal vessels form at a later developmental

stage.<sup>34</sup> Moreover, remodeling and enlargement of FAZ takes place after birth. It is also worth mentioning that neurons are an important source of vascular endothelial growth factor to control the development of the superficial and deep vascular plexus.<sup>35</sup>

Regarding macular thickness, previous studies have demonstrated conflicting results, with some investigations showing that the amblyopic eyes have increased macular thickness compared with fellow eyes,<sup>1,2,36</sup> or control eyes,<sup>1,2,4,36</sup> or no significant differences.<sup>3,10,30</sup> Our study demonstrated significantly greater overall macular thickness in amblyopic eyes compared with fellow eyes. Furthermore, analysis of the individual retinal layers showed that most inner retinal layers were thicker in amblyopic eyes, the previous reports on which have been somewhat inconsistent.<sup>6,31,37</sup> In terms of the outer retinal layers, the parafoveal outer segment photoreceptor/RPE complex (OPR), which presumably correlates with rod photoreceptor OS length in situ, was significantly thinner in amblyopic eyes compared with fellow eyes. A previous investigation has demonstrated that the length of OS in amblyopic eyes was shorter than that in fellow eyes at the fovea.<sup>5</sup> The current study, however, showed no difference in the length of OS between the paired eyes. However, the apparent contradiction may be reconciled by the fact that the OS length at the fovea reflects the elongated cone photoreceptor outer segments, whereas that outside the fovea reflects the length of the outer segments of the rod photoreceptor cells. The current results may raise the possibility that developmental abnormality in the process of foveal maturation is present in eyes with amblyopia. During foveal development, inner retinal neurons are displaced centrifugally to form the foveal pit and the cone cells are displaced centripetally, this produces a higher photoreceptor density with elongation of the inner and outer segments.<sup>38</sup> Recent histological and in vivo OCT studies have suggested that foveal development continues until around the middle teenage years rather than until 5 years of age as previously thought.<sup>38–42</sup> Lee et al.<sup>40</sup> found that foveal and parafoveal outer segments of photoreceptors show an increase in thickness with age until 45 and 145 months of the gestational period, respectively. We also identified positive correlations between age and foveal and parafoveal outer segment photoreceptors thickness in amblyopic eyes. Together with the findings of the current study and previous reports, we presume that disturbances in input of visual stimuli during early development may lead to retinal developmental abnormalities, at least in part.

We found negative correlations between macular thickness, especially in the inner retinal layers, and AL in both amblyopic and fellow eyes; however, in the analysis without magnification correction, the correlations were scattered and presented no identical pattern. Several previous studies have also reported negative correlations of AL with foveal RNFL and macular thickness in normal children,<sup>43–45</sup> whereas another found no such correlations.<sup>46</sup> Conversely, studies in adult cohorts have reported positive correlations between AL and foveal inner retinal layer thickness.<sup>16,47</sup> These conflicting results may reflect differences in macular structure according to the patient's age, race, sex, and refraction. Furthermore, as shown by our results, it is important to consider the measurement methods used, including with or without magnification correction. Moreover, it is speculated that the method used to adjust image size according to AL, such as Littman's formula, may also influence correlations among retinal parameters.

Visual acuity was not correlated with vessel densities or FAZ area. Because the foveal morphology in the normal human population shows substantial variations,<sup>38</sup> longitudinal studies are preferable for investigating the relationship between visual development and retinal structure in amblyopic eyes. One study detected an increase in photoreceptor OS length in amblyopic eyes after optical treatment.<sup>5</sup> Additionally, a large choroidal luminal area in anisohypermetropic amblyopic eyes was reportedly reduced after optical correction.<sup>48</sup> These findings suggest that neural activity of the retina is associated with the retinochoroidal structure. Further work should investigate the longitudinal changes in each retinal layer structure and macular vasculature during amblyopia treatment to help clarify the underlying pathophysiology of amblyopia.

### Limitations

This study has several limitations. First, a relatively small number of patients were enrolled, which may have led to failure in detecting an extant relationship during the correlation analyses. Second, we included patients with amblyopia in various treatment stages, and the resulting heterogeneity may have increased variation in some retinal parameters. However, examination of treatment-naïve pre-school patients is often challenging because fixation stability is necessary to ensure image quality. Third, there was no healthy control group for comparing the retinal structures. Nonetheless, the comparison with fellow eyes acts as an internal control, making it possible to detect the subtle differences without confounding factors that can influence values other than AL.

### CONCLUSION

This magnification-corrected OCT/OCTA imaging study revealed a reduction in both SCP and DCP macular vessel density and thicker inner retinal layers in amblyopic eyes. Changes in the macular microvasculature and structural layers may offer valuable insights into the development of amblyopia.

### Acknowledgments

Supported by Singapore Ministry of Health's National Medical Research Council under its Centre Grant Programme (NMRC/CG/C010A/2017 SERI).

Disclosure: **N. Nishikawa**, None; **J. Chua**, None; **Y. Kawaguchi**, None; **T. Ro-Mase**, None; **L. Schmetterer**, None; **Y. Yanagi**, None; **A. Yoshida**, None

### References

- Huynh SC, Samarawickrama C, Wang XY, et al. Macular and nerve fiber layer thickness in amblyopia: the Sydney Childhood Eye Study. *Ophthalmology*. 2009;116(6):1604–1609.
- Al-Haddad CE, Mollayess GM, Cherfan CG, Jaafar DF, Bashshur ZF. Retinal nerve fiber layer and macular thickness in amblyopia as measured by spectral-domain optical coherence tomography. *Br J Ophthalmol*. 2011;95(3):1696–1699.
- Atakan M, Culfa S, Calli U, Penbe AD, Atakan TG. Evaluation of retinal nerve fiber layer and macular thickness in amblyopia. *J Clin Exp Ophthalmol*. 2015;6(3):437.
- Bruce A, Pacey IE, Bradbury JA, Scally AJ, Barrett BT. Bilateral changes in foveal structure in individuals with amblyopia. *Ophthalmology*. 2013;120(2):395–403.
- Nishi T, Ueda T, Hasegawa T, Miyata K, Ogata N. Retinal thickness in children with anisohypermetropic amblyopia. *Br J Ophthalmol*. 2015;99(8):1060–1064.
- Chen W, Xu J, Zhou J, et al. Thickness of retinal layers in the foveas of children with anisometropic amblyopia. *PLoS One*. 2017;12(3):e0174537.
- Lonngi M, Velez FG, Tsui I, et al. Spectral-domain optical coherence tomographic angiography in children with amblyopia. *JAMA Ophthalmol*. 2017;135(10):1086–1091.
- Yilmaz I, Ocak OB, Yilmaz BS, Inal A, Gokyigit B, Taskapili M. Comparison of quantitative measurement of foveal avascular zone and macular vessel density in eyes of children with amblyopia and healthy controls: an optical coherence tomography angiography study. *J AAPOS*. 2017;21(3):224–228.
- Sobral I, Rodrigues TM, Soares M, et al. OCT angiography findings in children with amblyopia. *J AAPOS*. 2018;22(4):286–289.
- Chen W, Lou J, Thorn F, et al. Retinal microvasculature in amblyopic children and the quantitative relationship between retinal perfusion and thickness. *Invest Ophthalmol Vis Sci*. 2019;60(4):1185–1191.
- Araki S, Miki A, Goto K, et al. Foveal avascular zone and macular vessel density after correction for magnification error in unilateral amblyopia using optical coherence tomography angiography. *BMC Ophthalmol*. 2019;19(1):171.
- Wong ES, Zhang XJ, Yuan N, et al. Association of optical coherence tomography angiography metrics with detection of impaired macular microvasculature and decreased vision in amblyopic eyes: the Hong Kong Children Eye Study. *JAMA Ophthalmology*. 2020;138(8):858–865.
- Bennett AG, Rudnicka AR, Edgar DF. Improvements on Littmann's method of determining the size of retinal features by fundus photography. *Graefes Arch Clin Exp Ophthalmol*. 1994;32(6):361–367.
- Sampson DM, Gong P, An D, et al. Axial length variation impacts on superficial retinal vessel density and foveal avascular zone area measurements using optical coherence tomography angiography. *Invest Ophthalmol Vis Sci*. 2017;58(7):3065–3072.
- Linderman R, Salmon AE, Strampe M, Russillo M, Khan J, Carroll J. Assessing the accuracy of foveal avascular zone measurements using optical coherence tomography angiography: segmentation and scaling. *Transl Vis Sci Technol*. 2017;6(3):16.
- Chua J, Tham YC, Tan B, et al. Age-related changes of individual macular retinal layers among Asians. *Sci Rep*. 2019;9(1):20352.
- Llanas S, Linderman RE, Chen FK, Carroll J. Assessing the use of incorrectly scaled optical coherence tomography angiography images in peer-reviewed studies: a systematic review. *JAMA Ophthalmol*. 2019;138(1):86–94.
- Noval S, Freedman SF, Asrani S, El-Dairi MA. Incidence of fovea plana in normal children. *J AAPOS*. 2014;18(5):471–475.
- Linderman RE, Cava JA, Salmon AE, et al. Visual acuity and foveal structure in eyes with fragmented foveal avascular zones. *Ophthalmol Retina*. 2020;4(5):535–544.
- Schindelin J, Arganda-Carreras I, Frise E, et al. Fiji: an open-source platform for biological-image analysis. *Nat Methods*. 2012;9(7):676–682.
- Iafe NA, Phasukkijwatana N, Chen X, Sarraf D. Retinal capillary density and foveal avascular zone area are age-dependent: quantitative analysis using optical coherence

- tomography angiography. *Invest Ophthalmol Vis Sci.* 2016;57(13):5780–5787.
22. Ishii H, Shoji T, Yoshikawa Y, Kanno J, Ibuki H, Shinoda K. Automated measurement of the foveal avascular zone in swept-source optical coherence tomography angiography images. *Transl Vis Sci Technol.* 2019;8(3):28.
  23. Domalpally A, Danis RP, White J, et al. Circularity index as a risk factor for progression of geographic atrophy. *Ophthalmology.* 2013;120(12):2666–2671.
  24. Otsu N. A threshold selection method from gray-level histograms. *IEEE Trans Syst Man Cybern Syst.* 1979;9:62–66.
  25. Ro-Mase T, Ishiko S, Omae T, Ishibazawa A, Shimouchi A, Yoshida A. Association between alterations of the choriocapillaris microcirculation and visual function and cone photoreceptors in patients with diabetes. *Invest Ophthalmol Vis Sci.* 2020;61(6):1–9.
  26. Sohn EH, Chen JJ, Lee K, Niemeijer M, Sonka M, Abramoff MD. Reproducibility of diabetic macular edema estimates from SD-OCT is affected by the choice of image analysis algorithm. *Invest Ophthalmol Vis Sci.* 2013;54(6):4184–4188.
  27. Terry L, Cassels N, Lu K, et al. Automated retinal layer segmentation using spectral domain optical coherence tomography: evaluation of inter-session repeatability and agreement between devices. *PLoS One.* 2016;11(9):e0162001.
  28. Kanda Y. Investigation of the freely-available easy-to-use software EZR for medical statistics. *Bone Marrow Transplant.* 2013;48(3):452–458.
  29. Odell D, Dubis AM, Lever JF, Stepien KE, Carroll J. Assessing errors inherent in OCT-derived macular thickness maps. *J Ophthalmol.* 2011;2011:692574.
  30. Lekskul A, Wuthisiri W, Padungkiatsagul T. Evaluation of retinal structure in unilateral amblyopia using spectral domain optical coherence tomography. *J AAPOS.* 2018;22(5):386–389.
  31. Araki S, Miki A, Goto K, et al. Macular retinal and choroidal thickness in unilateral amblyopia using swept-source optical coherence tomography. *BMC Ophthalmol.* 2017;17(1):167.
  32. Doguizi S, Yilmazoglu M, Kiziltoprak H, Sekeroglu MA, Yilmazbas P. Quantitative analysis of retinal microcirculation in children with hyperopic anisometropic amblyopia: an optical coherence tomography angiography study. *J AAPOS.* 2019;23(4):201.e1–201.e5.
  33. Karabulut M, Karabulut S, Sül S, Karalezli A. Microvascular changes in amblyopic eyes detected by optical coherence tomography angiography. *J AAPOS.* 2019;23(3):155.e1–155.e154.
  34. Provis JM, Hendrickson AE. The foveal avascular region of developing human retina. *Arch Ophthalmol.* 2008;126(4):507–511.
  35. Joyal J-S, Gantner ML, Smith LEH. Retinal energy demands control vascular supply of the retina in development and disease: the role of neuronal lipid and glucose metabolism. *Prog Retin Eye Res.* 2018;64:131–156.
  36. Rajavi Z, Sabbaghi H, Behradfar N, Yaseri M, Aghazadeh Amiri M, Faghihi M. Macular thickness in moderate to severe amblyopia. *Korean J Ophthalmol.* 2018;32(4):312.
  37. Firat PG, Ozsoy E, Demirel S, Cumurcu T, Gunduz A. Evaluation of peripapillary retinal nerve fiber layer, macula and ganglion cell thickness in amblyopia using spectral optical coherence tomography. *Int J Ophthalmol.* 2013;6(1):90–94.
  38. Bringmann A, Syrbe S, GÖrner K, et al. The primate fovea: structure, function and development. *Prog Retin Eye Res.* 2018;66:49\*84.
  39. Dubis AM, Costakos DM, Subramaniam CD, et al. Evaluation of normal human foveal development using optical coherence tomography and histologic examination. *Arch Ophthalmol.* 2012;130(10):1291–1300.
  40. Lee H, Purohit R, Patel A, et al. In vivo foveal development using optical coherence tomography. *Invest Ophthalmol Vis Sci.* 2015;56(8):4537–4545.
  41. Yuodelis C, Hendrickson A. A qualitative and quantitative analysis of the human fovea during development. *Vision Res.* 1986;26(6):847–855.
  42. Vajzovic L, Hendrickson AE, O'Connell RV, et al. Maturation of the human fovea: correlation of spectral-domain optical coherence tomography findings with histology. *Am J Ophthalmol.* 2012;154(5):779–789.
  43. Huynh SC, Wang XY, Rohtchina E, Mitchell P. Distribution of macular thickness by optical coherence tomography: findings from a population-based study of 6-year-old children. *Invest Ophthalmol Vis Sci.* 2006;47(6):2351.
  44. El-Dairi MA, Asrani SG, Enyedli LB, Freedman SF. Optical coherence tomography in the eyes of normal children. *Arch Ophthalmol.* 2009;127(1):50–58.
  45. Cheng L, Wang M, Deng J, et al. Macular ganglion cell-inner plexiform layer, ganglion cell complex, and outer retinal layer thicknesses in a large cohort of Chinese children. *Invest Ophthalmol Vis Sci.* 2019;60(14):4792–4802.
  46. Lim ME, Jiramongkolchai K, Xu L, et al. Handheld optical coherence tomography normative inner retinal layer measurements for children <5 years of age. *Am J Ophthalmol.* 2019;207:232–239.
  47. Palazon-Cabanes A, Palazon-Cabanes B, Rubio-Velazquez E, Lopez-Bernal MD, Garcia-Medina JJ, Villegas-Perez MP. Normative database for all retinal layer thicknesses using SD-OCT posterior pole algorithm and the effects of age, gender and axial length. *J Clin Med.* 2020;9(10):3317.
  48. Nishi T, Ueda T, Mizusawa Y, et al. Effect of optical correction on choroidal structure in children with anisohypermetropic amblyopia. *PLoS One.* 2020;15(4):e0231903.